High efficiency rectifier for a variable speed transverse flux permanent magnet generator for wind turbine applications

Mehdi Taghizadeh Kakhki, Maxime R. Dubois
Université Laval
1065 Ave de la Médecine
Québec (PQ) G1V 0A6, Canada
Tel.: +1/ (418) – 656-2131
Fax: +1 / (418) – 656-3159
E-Mail: mehdi.taghizadeh.1@ulaval.ca
URL: http://www.ulaval.ca

Keywords

High efficiency rectifier, Transverse flux machine, Wind turbine.

Abstract

An uncontrolled bridge rectifier could not be used with a transverse flux machine due to its high stator reactance. A high efficiency rectifier topology is introduced which could be used with sources with variable frequency and high source inductance including transverse flux machines.

Introduction

Due to its interesting characteristics including its high torque density, transverse flux permanent magnet machine (TFPM) could be considered as an interesting choice for a wind energy conversion system. Transverse Flux PM machines can achieve very high torque density at low rotational speeds, which is especially relevant in applications such as direct-driven wind turbine generators [1]. Such high torque/volume ratio is achievable with the documented disadvantage of TFPM machines having a high stator reactance (X_s between 1.5 and 3 p.u. can be expected). The presence of high stator reactance in a synchronous generator will lead to a limitation in the extractable output power of an uncontrolled diode rectifier in both current source and voltage source rectifiers. As a solution, PWM rectifiers using IGBTs could be used which are well adapted to variable frequency sources with high input inductance, however, they have high conduction losses which will result in low efficiencies particularly at high source currents and their switching losses will also lower the efficiency particularly at low loads. As an alternative, a bi-directional magnetic recovery switch (MERS) is proposed in [2] which could provide series active compensation for the synchronous reactance. However in this type of compensation, the total stator current will have to pass through the two series IGBTs which conduction losses add to the accompanying diode rectifier. The results for power losses (calculation) in [3] show that this topology (in the context of a wind power conversion system) will yield a better efficiency compared to a system using a PWM rectifier. However, it should be noticed that, in this comparison, an important part of the difference in efficiency is due to the losses in the input inductance (for the PWM rectifier) which efficacy and rating could be questioned.

In this article an AC/DC converter topology will be introduced which could be considered as a high-efficiency alternative to above-described topologies, when applied to a variable speed wind energy conversion system. This new rectifier configuration is named the Rapid Polarity Reversal (RPR) Rectifier. To examine the feasibility of employing such a RPR converter in direct-drive wind turbines, the power curve for a MW range turbine, will be used along with numerical analysis to establish its efficiency-speed curves and will then be compared to the simulation results for a two-level IGBT-based Sine-PWM rectifier with identical turbine power curves. The annual energy production of the

turbine for both converter options and their respective initial investment has been compared to see if it is economically justified to employ the RPR rectifier for a MW range wind turbine with a TFPM generator. Finally, an experimental model of the proposed topology is presented.

Analysis of the Rapid Polarity Reversal Rectifier

Fig. 1 shows the Rapid Polarity Reversal (RPR) converter for a constant current load I_{out}. It allows a rapid reversal of the current polarity in a TFPM machine despite its large value of stator inductance L_g. A variety of switches may be used for S1-S4 in fig.1 including thyristors, IGBTs, IGCTs, etc.. While natural commutation is possible for S3 and S4, it can be shown that S1 and S2 must be forced-commutated switches. Fig. 2 shows the source EMF voltage (e_g), Source Current (i_{Lg}), Capacitor Voltage (v_C) and Capacitor current (i_C) for the RPR converter. Fig. 3 shows the current path for each time sequence (0 to 3). During the resonance mode in interval 1, the energy stored in the source inductance L_g will be transferred to the capacitor C, enabling the generator current to fall to zero very quickly. At this point of zero generator current, capacitor C will be charged to its maximum value (V_{Cmax}). During interval 2 the energy stored in the capacitor will be transferred to the source inductance, enabling a fast polarity reversal of the source current i_{LG}. Generating the proper trigger pulse pattern for switches S3 and S4 of the RPR converter is a straight forward task, although care must be taken in order to avoid any disruption in the source current.

In order to maximize the power output and minimize V_{Cmax} , the charging time of the capacitor should be anticipated so that V_{Cmax} coincides with the zero crossing of the EMF voltage (t_1) (which is detected by a rotary encoder). This function can easily be implemented with a microcontroller. The charging time of the capacitor is the difference $t_1 - t_0$ (see fig. 2), which value will depend upon the values of L_g and C, but also upon the generator voltage E and current I_{LG}. As mentioned, suitable calculation of that charging time is key to the RPR rectifier. During the polarity reversal process of interval 1, the inductor current I_{LG} at the end of a half cycle of resonance (I_1) will be different from its initial value (I_0) by ΔI_{Lg}, as shown in Eq (1), In this case, a constant output current (I_{Out}) is considered. Thus, the commutation between the two thyristors (T2 and T4 in the transition from interval 2 to 3) will depend on ΔI_{Lg} only.

$$\Delta I_{Lg} = |I_1| - |I_0| = -|I_0| \frac{\alpha\pi}{\omega_r} + 2CE\omega_g \qquad (1)$$

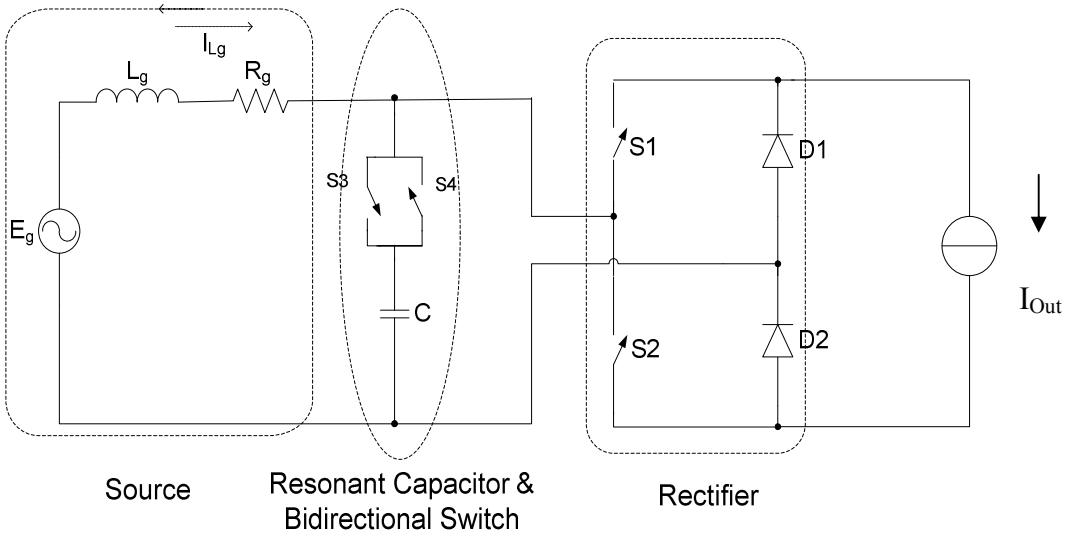

Fig. 1: RPR rectifier

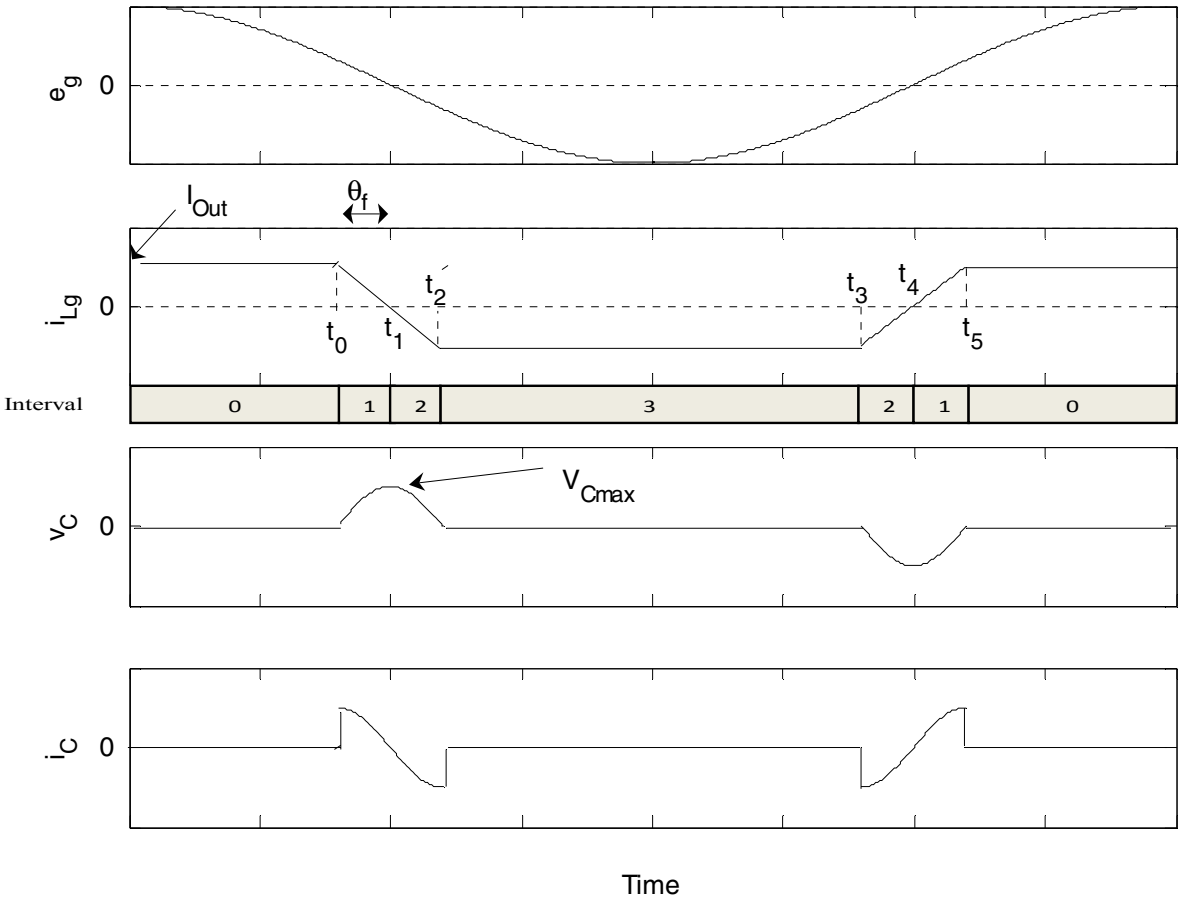

Fig. 2: Source EMF voltage (e_g), Source Current (i_{Lg}), Capacitor Voltage (v_C) and Capacitor current (i_C) for the RPR converter

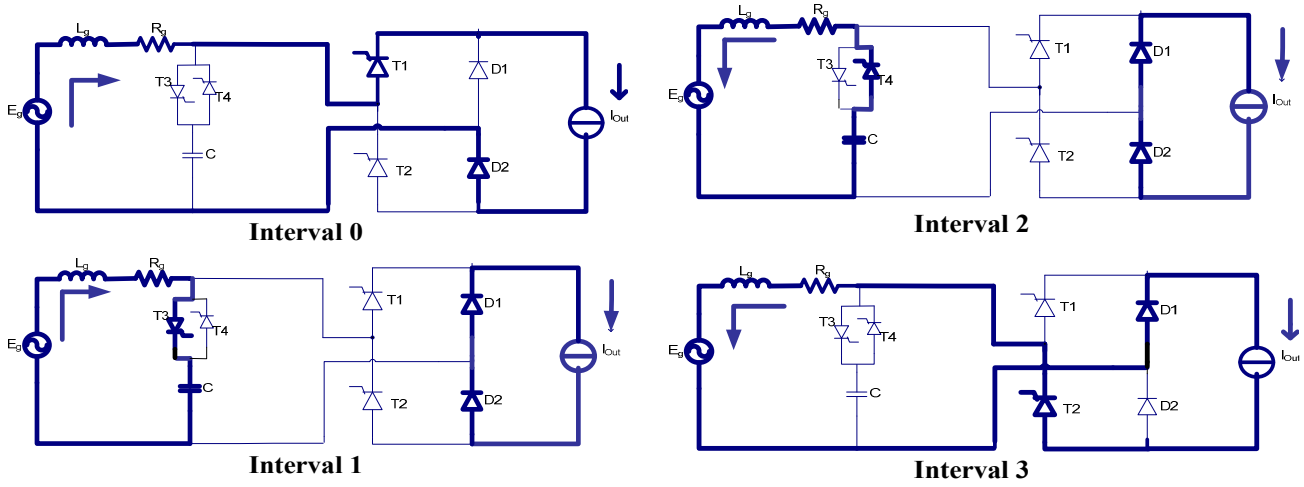

Fig. 3: Current path (for intervals 0 to 3)

Where $\omega_r = \sqrt{{\omega_0}^2 - \alpha^2}$, $\omega_0 = \frac{1}{\sqrt{L_g C}}$, ω_g is angular frequency of the generator EMF, E is the peak value of the generator EMF, and α is the damping factor. In this paper, the value of L_g is assumed to be constant. However, it must be noted that saturation of the TFPM magnetic circuit will introduce inevitable variations in the value of Lg, leading to variations in the value of wr and w0. This difficulty can be circumvented by updating the values of L_g, ω_r and ω_0 by implementing a look-up table within

the controller algorithm, as discussed in [4]. The term $2CE\omega_g$ in equation (1) represents the effect of the source EMF voltage while the term $-|I_0|\frac{\alpha\pi}{\omega_r}$ shows the effect of damping on the initial inductor current after a half cycle,. This may result in an additional commutation time in a circuit with high damping factor , however in a TFPM machine it will not be considerable due to its low damping factor ($\alpha << \omega_0$).

Assuming constant load current (I_{Out}), sinusoidal generator EMF and no generator losses, we can express the output power of the converter as follows [4]:

$$P_{Out} = \frac{2}{\pi} E I_{L\,g,nom} \frac{\cos(\theta_f)}{\sqrt{1-(\frac{4}{3}\frac{\theta_f}{\pi})}} \tag{2}$$

where θ_f is the firing angle $\omega_g(t_1\text{-}t_0)$. Increasing θ_f will lower the displacement factor (DISF) of the source current (represented by the term $\sqrt{1-(\frac{4}{3}\frac{\theta_f}{\pi})}$) and decrease the output voltage (represented by the term $\frac{2}{\pi} E\cos(\theta_f)$).

The output power of the RPR converter normalized to that of the ideal diode rectifier is shown in equation (3):

$$P_{Out\,(Norm)} = \frac{\cos(\theta_f)}{\sqrt{1-(\frac{4}{3}\frac{\theta_f}{\pi})}} \tag{3}$$

For a constant output current I_{out}, the peak capacitor voltage will be:

$$V_{C\max} = I_{out}\sqrt{\frac{L_g}{C}} \tag{4}$$

As shown in [4], the total current harmonic distortion (TCHD) of the generator current is given:

$$TCHD = \sqrt{1-(\frac{8\cos^2(\theta_f)}{\pi^2 - \frac{4}{3}\theta_f\pi})}100\% \tag{5}$$

Rectifier Losses

This section will focus on the efficiency of the RPR rectifier, which is needed for an accurate comparison with the PWM rectifier, further in the paper. Here, we are assuming switches S1 and S2 to be IGCTs, switches S3 and S4 to be thyristors and D1, D2 to be diodes. For low operating frequencies, thyristor and diode conduction losses will dominate and switching losses will be ignored. Conduction losses in a switch can be expressed as follows:

$$P_{SW} = \frac{1}{T}\int_0^T v_F(t) i_{on}(t)\,dt \tag{6}$$

where v_F and i_{on} are the instantaneous forward voltage and current in the switch. Some manufacturers like ABB provide an "on-state characteristic model" for some of their thyristors and diodes which could be used for a more precise loss calculation, otherwise the linear model for the thyristors and diodes, will give a reasonable accuracy. For a constant load current, the losses in the thyristor half bridge could be calculated as follows:

$$P_{T1-T2} = \frac{\pi - 2\theta_f}{\pi}(I_{out}V_{T0,T1-T2} + I^2{}_{out}r_{on,T1-T2}) \tag{7}$$

where V_{T0} is the threshold voltage and r_{on} is the on-state resistance of the switch and the subscript "T1-T2" represents the thyristors in the controlled half-bridge.

The conduction losses for both diodes during resonance will be:

$$P_D = \frac{4\theta_f}{\pi}(I_{out}V_{F0,Diode} + I_{out}{}^2 r_{on,Diode}) \tag{8}$$

where the subscript "Diode" represents the diodes in the diode half-bridge.

During normal conduction mode, the loss equation for the diodes will be similar to Eq. (7), so the total diode losses will be:

$$P_D = \frac{\pi + 2\theta_f}{\pi}(I_{out}V_{F0,Diode} + I_{out}{}^2 r_{on,Diode}) \tag{9}$$

The conduction losses in the bidirectional switch could be expressed as:

$$P_{T3-T4} = 2\frac{\theta_f}{\pi}I_{out}^2\left(\frac{V_{T0,T3-T4}}{\pi I_{out}} + \frac{1}{2}r_{on,T3-T4})\right) \tag{10}$$

where the subscript "T3-T4" represents the thyristors in the bidirectional switch.

Losses in the capacitor will be:

$$P_C = I_{out}{}^2\frac{\theta_f}{\pi}ESR_C \tag{11}$$

where ESR_C is the Equivalent Series Resistance of capacitor C.

As expected, as θ_f increases, the losses in the thyristor half-bridge will decrease, while losses in the diode half-bridge, bi-directional switch and capacitor will increase. Increasing output current will have a more pronounced effect on the capacitor loss.

Comparison with PWM rectifier in the MW range

A turbine design (rated mechanical rotor power of 3.3 MW, rotor diameter of 90 m, with a speed of 16 rpm at rated wind (10 m/s)) [6] was considered for the analysis (fig. 4).

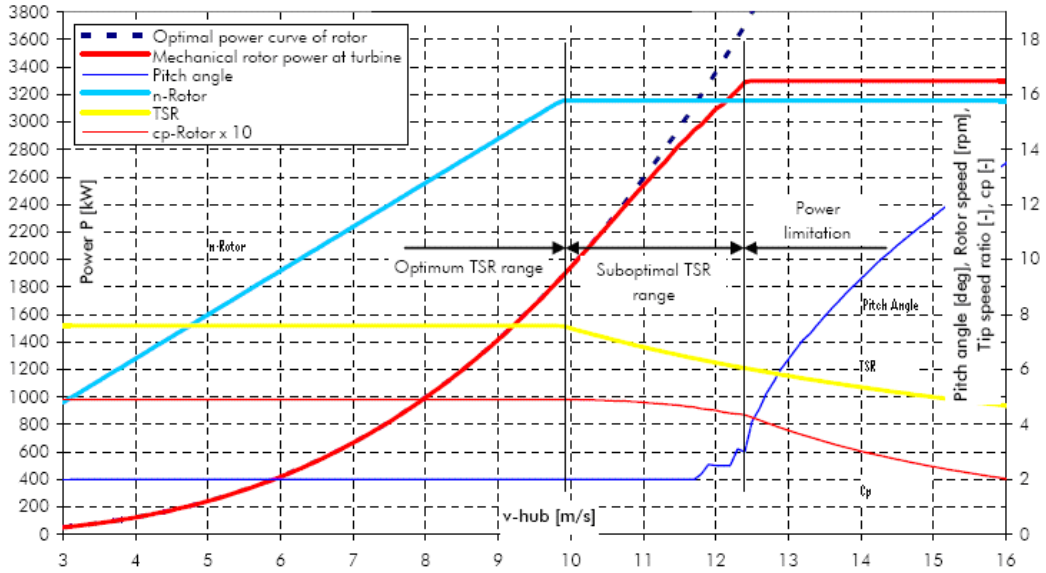

Fig. 4: Power curve for a 3.3 MW wind turbine [6].

The mechanical and electrical losses in the generator were not taken into account. It was assumed that the turbine power will be equally divided between three transverse flux machines sharing the same shaft. It should be noted that TFPM machine is basically a single-phase machine (though it is possible to build multi-phase machines by using independent single-phase units sharing the same shaft).

Analytical formulas were used in an Excel based simulation tool to calculate the semiconductor losses for the RPR rectifier in the MW range assuming a sinusoidal EMF. Knowing the desired power curve, the current curve of the machine versus wind speed was established. The Diode and thyristor specifications and rectifier maximum output current will impose the value for capacitor C, which will, in turn, imposes the firing angle (θ_f) for each wind speed.

The IGCT version was used which is less efficient and costs more than the thyristor version, however it does not need a forced commutation circuit (FCC) and can be easily realized and evaluated due to its simplicity. Table 1 shows the specifications for each single phase generator-Rectifier (1 MW) the at rated wind speed (12.5 m/s). The IGCTs, their reverse blocking diodes (RB-Diodes) and the two freewheeling diodes were overrated mainly due to the very limited choice of switches at these ratings particularly for the IGCTs. The efficiency reaches its peak value when generator speed reaches its nominal value (16 rpm) at a wind speed equal to 10 m/s. Fig. 5 shows the distribution of losses in the rectifier at this point.

For the PWM rectifier it was assumed that the turbine power is equally distributed among three conventional 3-phased two-level PWM VSI converters (3x3-phase 1MW PWM VSI converter is considered as an economic and efficient option for this power range, that is why a VSI rather than a CSI converter is considered). The 3-phased generators have the same line-neutral EMF voltage versus rotor speed ($E_g = \frac{690}{\sqrt{3}} @ 16\,rpm$) and the same reactance (X_g=2 p.u.). For loss calculation in PWM converters, a simulation tool from ABB [5] was employed. The switching frequency was chosen to be a rather low value (1 kHz compared to 5 kHz in [3]). Unlike [3] only semiconductor losses were considered in the PWM converter.

The resulting efficiencies are compared in Fig. 6. As could be seen for the RPR-converter, the efficiency will be high for the whole range of wind speeds in contrast to PWM rectifiers where efficiency falls to very low values as the wind speed decreases (below 10 m/s). The share of bidirectional switch and capacitor losses will drastically decrease at lower output powers, where the resonance interval will be smaller compared to normal conduction interval. The same power curve and the two sets of efficiency characteristics for the RPR and PWM converters were used to compare the annual energy production of the two topologies (PWM and the RPR rectifiers) and calculate the total

energy savings. The Rayleigh distribution with an average annual wind speed equal to 7 m/s was used to approximate the wind speed probability as shown in fig. 7(c). The results of the calculation at each wind speed is shown in fig. 7 (b).The amount of energy saved with the new topology at each wind speed is shown in fig. 7 (c).

Table 1. 1 MW generator-Rectifier specifications at rated wind speed (12.5 m/s).

Power components:		Source EMF, RMS, E_g	(V)	$\frac{690}{\sqrt{3}}$
IGCT for S1,S2:	5SHY 35L4512	Source reactance, X_g	pu	2
RB-Diode for S1,S2:	5SDD 50N5500	Number of pole pairs, p		122
Diode for D1,D2:	5SDA 27F2002	Output current, I_{Out}	(A)	2934

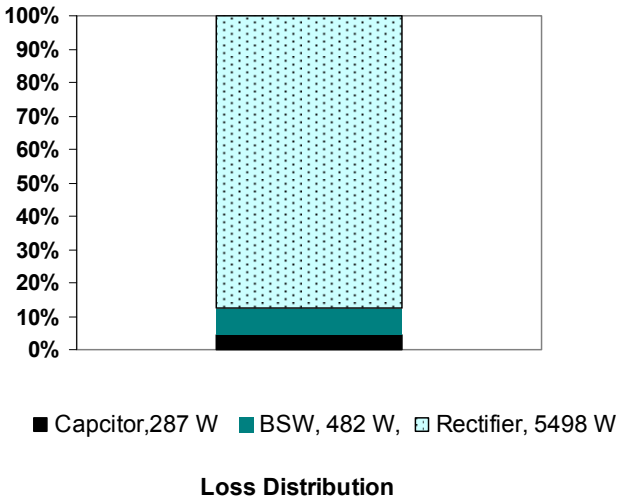

Fig. 5: Loss distribution at 10m/s, P_{Out}=598 kW

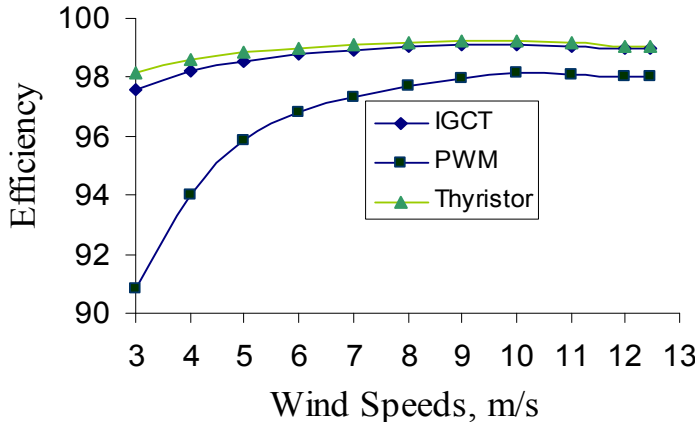

Fig. 6: The efficiency of the PWM rectifier versus the IGCT and thyristor (FCC losses not included) versions of the RPR rectifier.

The semiconductor prices for the two topologies are compared in table 2. The semiconductor prices for RPR topology were obtained directly from ABB. It was found that the extra investment required is less than 9 percent of the economies made. This rather rough evaluation based on the rectifier losses only is intended to give a general idea of the extra investment required and should be followed by a more comprehensive comparison where the whole energy conversion system (including

the generator, EMI and dc-link filters) are considered. In this case, an increase in magnetic losses for a machine fed by a PWM converter and different filtering needs should be also evaluated.

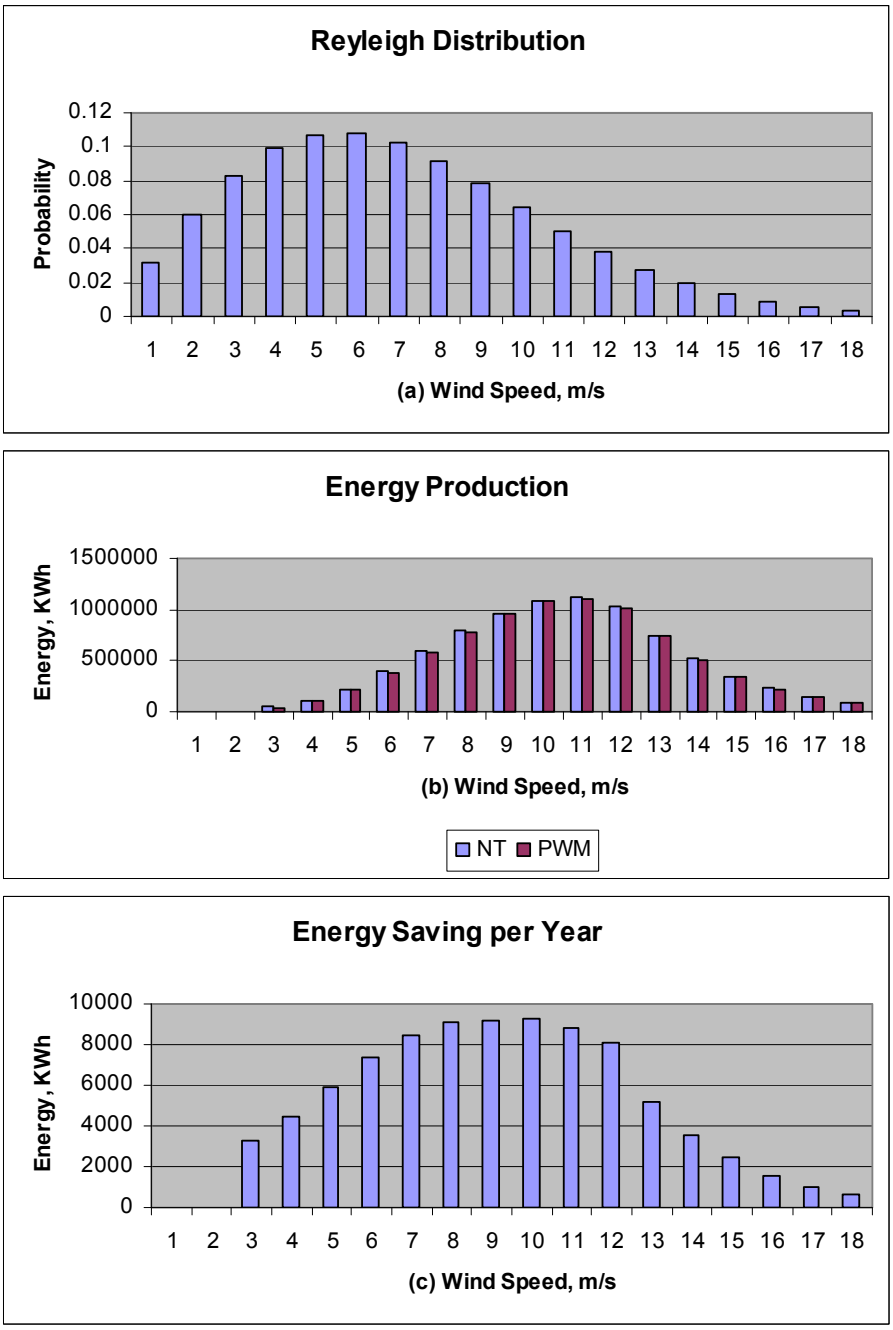

Fig. 7 (a) Rayleigh distribution for an average wind speed of 7 m/s, (b) annual energy production of the turbine at each wind speed, (c) energy saved with the new topology (NT) at each wind speed per year.

Table 2

Semiconductors (PWM)	USD	15147
Semiconductors + Cap. (RPR)	USD	26751
Extra Investment Required	USD	11603
Energy Saving in 20 Years	KWh	1760980
Energy Saving @0.07$/KWh	USD	123269

Experimental Results

An experimental low voltage low power model of the RPR-converter was built whose specifications are shown in table 3. The source inductance was made of two parallel laminated core inductances. Thyristors were used in the controlled half-bridge (for T1 and T2) as shown in fig. 8. Synchronization was implemented using a zero-crossing detector. No particular consideration was taken for the choice of input voltage . As far as Load parameters are concerned, the load resistance (R) was adjusted to obtain the required input current (for a reactance of X_g=2.36 pu). Due to high core losses in the laminated core inductance (L_g), and low input voltage, ΔI_{Lg} in Eq. (1) will not be negligible. The choice of the load reactance was made for a minimal commutation time. This will not apply to a TFPM due to much lower damping factor. It should be also emphasized that this low power model is only meant to show the feasibility of the converter. The commutation circuit is not recommended for a MW range converter where IGCTs or more efficient FCCs might be used. Fig. 9 shows the waveforms for source voltage and source current.

Table 3

L_g	$E_{g\ (no\ load)}$	I_{nom}	f	θ_f
pu	V	A	Hz	Deg.
2.36	15.56	7.07	60	8.4

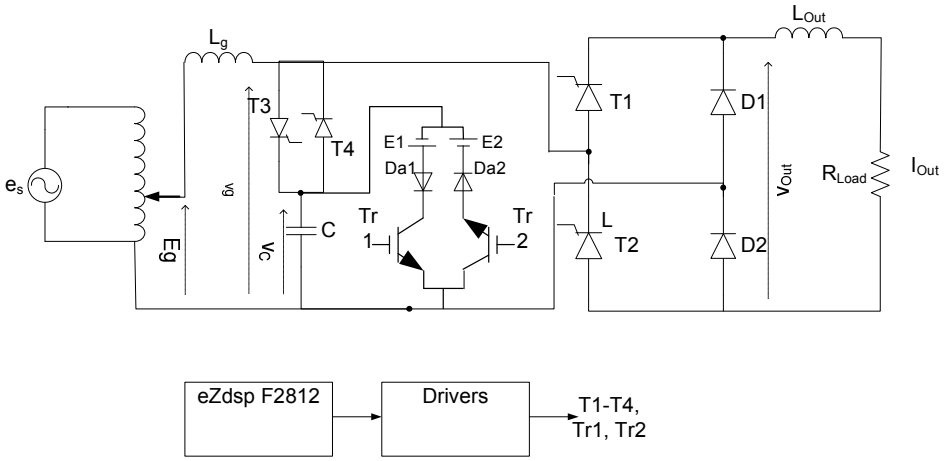

Fig.8: The experimental circuit

Table 4 presents the results for the loss distribution in different components of the RPR-converter by the simulation tool for the same output power and output current. The efficiency was 1.9% higher than the measured value. This deviation could be partly explained by the losses due to FCC, ripple in the output current, and the fact that thyristor and diode model parameters are only approximate values due to unknown junction temperatures.

Discussion

The simulation with simulink and the experimental results confirm that the RPR converter could be used with sources with high reactance. It was also shown that the RPR rectifier is superior to a PWM VSI two-level rectifier at low loads and considerably more efficient at all load and frequencies (wind speeds). Due to higher efficiencies, cooling requirements for the switches are also lower. Core saturation does not affect the functionality of the RPR rectifier and it requires no dv/dt snubber (no snubber losses) since dv/dt will be determined by the voltage across the capacitor C.

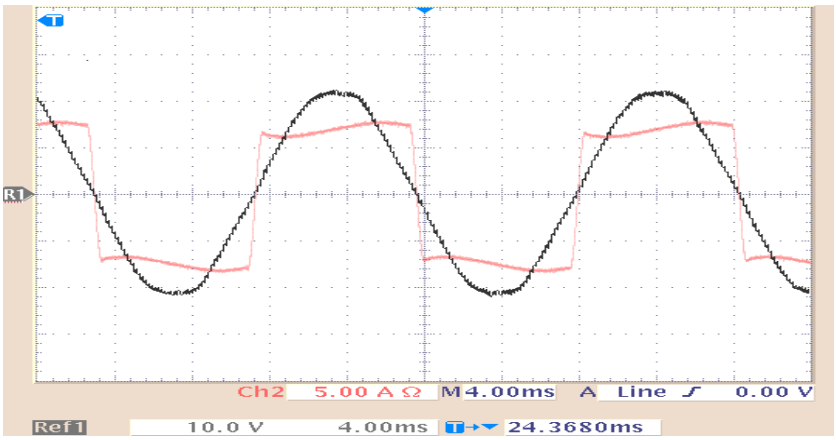

Fig.9 : Source voltage (eg, CH1), source current (iLg, CH2), Xg=2.36 pu

Table 4. Loss distribution in different components of the RPR-converter (simulation tool)

D-HB	Thy-HB	BSW	Capacitor	FCC
4.84 W	6.67 W	0.39 W	0.02 W	0.26 W

Since the choice of capacitor C will impose the V_{Cmax} and the resonance period, its value should be rather selected based on a compromise between these two parameters. This will limit the use of this rectifier at high frequencies where the turn-off time (t_q) of the thyristor and high values of V_{Cmax} will make it unpractical. However, it was shown that for a MW range wind turbine, despite the lower switch utilization in the RPR compared to PWM converter, the economy in energy due to lower converter losses is much more important than the extra initial investment required due to higher switch ratings. In the case of a trapezoidal EMF, the capability to control the trapezoidal current slope will be a definite advantage, since by increasing the resonance period, the torque could maximized and V_{Cmax} could be minimized. Due to approximations in the modeling of the semiconductors in the simulation tools, an experimental set up with higher ratings for both converters (RPR and PWM) using the same TFPM machine is suggested to validate the simulation results. The torque ripple and the effect of active power control on rectifier characteristics should be also further studied.

References

[1] M. R. Dubois, “Optimized permanent magnet generator topologies for direct-drive wind turbines”, PhD thesis, Delft University of Technology, 2004.

[2] K. Shimada et al: “Bi-directional current switch with snubber regeneration using P-MOSFETs,” in Proc. International Power Electronics Conference, Apr. 2000, no. 3, pp. 1519–1524.

[3] Takaku, T. Homma, G. Isobe, T. Igarashi, S. Uchida, Y. Shimada, R., “Improved Wind Power Conversion System Using Magnetic Energy Recovery Switch (MERS)”, CONFERENCE RECORD OF THE IEEE INDUSTRY APPLICATIONS CONFERENCE, 2005, VOL 40; PART 3, pages 2007-2012.

[4] M. T. Kakhki, “Rectifier Solutions for a Transverse Flux Permanent Magnet Machine”, Msc dissertation, Université Laval, 2008.

[5] P.J. Van Duijsen, P. Bauer, U. Killat, " Realistic benchmarking of IGBT-modules with the help of a fast and easy to use simulation-tool ", PCIM 04, Nurnberg, revised 01.07.05.

[6] A. Kantelberg, “On the influence of Design Tip Speed Ratio on Turbine Performance”, Paper, http://www.euros.de/On_the_Influence_of_TSR-opt.pdf